MAY 1980

PPPL-1663
UC-20g

N-DEPENDENCE OF BALLOONING INSTABILITIES

BY

R. L. DEWAR, J. MANICKAM, R. C. GRIMM, AND M. S. CHANCE

PLASMA PHYSICS LABORATORY

PRINCETON UNIVERSITY
PRINCETON, NEW JERSEY

This work was supported by the U.S. Department of Energy Contract No. DE-AC02-76-CHO 3073.

n-Dependence of Ballooning Instabilities

R. L. Dewar, J. Manickam, R. C. Grimm, and M. S. Chance

Plasma Physics Laboratory, Princeton University

Princeton, New Jersey 08544

The critical β for stability against ideal hydromagnetic internal ballooning modes as a function of toroidal mode number, n, is calculated for two different equilibrium sequences by use of a finite element technique ($n \lesssim 20$), and a WKB formalism ($n \gtrsim 5$). The agreement between the two methods is good in the overlap region $5 \lesssim n \lesssim 20$. The WKB formula reduces to the "1/n correction" at very high n, but is much more accurate at moderate n. The critical β vs n curves exhibit oscillatory structure at low n, but in both sequences the lower bound on β_c is set by $n = \infty$ modes at about $\beta_c \sim 5\%$. For reactor parameters, finite Larmor radius effects are not expected to have a large effect on this β-limitation.

I. INTRODUCTION

Doubt has recently [1] been cast on the relevance of $n = \infty$ stability limits found by application of the ideal hydromagnetic ballooning mode formalism [2-5]. This arose from the discrepency between the critical β ($\beta_c \equiv 2 \int p\, d\tau / \int B_\phi^2\, d\tau$, at marginal stability) found by extrapolation of low toroidal mode number, n, results to $n = \infty$ (giving $\beta_c \sim 10\%$), and the strictly $n = \infty$ result of the ballooning mode method (giving $\beta_c \sim 5\%$). On the basis of the 1/n correction formula [5,6] derived from ballooning mode theory, it was argued that the much more pessimistic ballooning results did not become valid until n was as high as 150. At such high values of n, it was suggested that nonideal effects might stabilize the modes.

In order to clarify the role of high n modes, it is necessary to obtain quantitative results in the region $n \gtrsim 5$. We have done this using two complementary techniques: a new finite element code (PEST-II [7]), good for $n \lesssim 20$, and a new [6,8] WKB technique for ballooning modes, good for $n \gtrsim 5$.

The two techniques agree well in their region of overlap, whereas the 1/n correction formula [5,6] is sensitive to the normalization used for δW, and can give very inaccurate results. For instance, at $\beta = 10\%$, in the case cited in Ref. 1, we find instability for $n \gtrsim 21$. With typical reactor parameters [9], this would give $k_\perp \rho_i \sim 0.1 - 0.2$, so finite Larmor radius effects cannot be counted on to stabilize ballooning modes at $\beta \sim 10\%$, and the lower limit set by $n = \infty$ stability is probably more realistic. We have also found that the function $\beta_c(n)$ has considerable structure at low n, implying that extrapolation based on a few integer values of n is not a valid procedure.

We now describe the choice of equilibrium sequences, the *PEST-II* and *WKB* calculations, and give an explanation for the breakdown of the $1/n$ formula.

II. EQUILIBRIUM SEQUENCES

We have studied two sequences of equilibria in which β varies continuously from 0% to > 20%. Sequence I was obtained by applying a flux conserving algorithm [10] to a D-shaped equilibrium with an aspect ratio of 4.0, minor radius = 1.25 m, elongation = 1.65, and "deeness" of 0.5. The values of the safety factor (q) on the magnetic axis and plasma surface were $q_o = 1.0$ and $q_s = 2.0$, respectively. The pressure profile was as described in Ref. 1.

Sequence II was obtained by selecting the case $\beta = 21\%$ from Sequence I, and from it generating a family of equilibria, parameterized by a scaling parameter s, such that the pressure and poloidal field remain invariant, while the toroidal field $B_\phi(\vec{x}|s)$ is related to that in the base case, $B_\phi(\vec{x}|1)$, by the equation

$$X^2B_\phi^2(\vec{x}|s) = X^2B_\phi^2(\vec{x}|1) + (s^2 - 1)\ R^2B_o^2 \quad , \tag{1}$$

which ensures that the Grad-Shafranov equation remains satisfied

[11]. Here X is the distance from the major axis, while RB_o is the value of XB_ϕ on the surface of the plasma. This sequence is characterized by constant poloidal β ($\beta_p \equiv 2 \int p\, d\tau / \int B_p^2\, d\tau = 2.5$), and higher q and q' at lower values of $\beta(s) \approx \beta(1)/s^2 = 21\%/s^2$. Sequence II reproduces fairly accurately [12] the one used to produce Fig. 6 of Ref. 1, but in order to suppress the complicating factor of surface kink modes we treat the case of a conducting wall on the plasma boundary. Thus our low-n results are even more optimistic than those of Ref. 1.

III. COORDINATE SYSTEM

We use a (ψ, θ, ζ) coordinate system, where 2πψ is the poloidal flux, θ is an arbitrary poloidal angle, and ζ is a toroidal angle chosen so that the magnetic field lines are straight in (θ,ζ) space. Thus,

$$\vec{B} = \vec{\nabla}\zeta \times \vec{\nabla}\psi + q(\psi)\, \vec{\nabla}\psi \times \vec{\nabla}\theta \,, \tag{2}$$

so $\vec{B}\cdot\vec{\nabla} = J^{-1}(\partial_\theta + q\partial_\zeta)$,
where $J \equiv (\vec{\nabla}\psi \times \vec{\nabla}\theta\cdot\vec{\nabla}\zeta)^{-1}$.

If ζ is the usual toroidal angle ϕ, then our poloidal angle θ is that of the PEST-I stability code [13], and the Jacobian is given by $J = X^2/\alpha(\psi)$, where α(ψ) is determined by periodicity requirements. This choice has the undesirable feature for numerical work at high β, that an equally spaced θ-grid becomes very coarse in real space near the outside region where the poloidal field is high. For integrating the ordinary differential equation arising *in the ballooning mode formalism* [2-5], the choice $J = X/[\alpha(\psi)|\vec{\nabla}\psi|]$, which gives equal arc lengths on the intersection of a magnetic surface with the plane $\phi = const$, *has been found to* be optimal. The current PEST-II calculations were done with $J = X^2/\alpha(\psi)$, which was found to give adequate accuracy with the number of Fourier modes used. The effect of other choices of Jacobian on convergence is under investigation.

IV. PEST-II

The essential difference between *PEST-I [13] and PEST-II is* the use in PEST-II of a model kinetic energy density $(1/2)\rho\omega^2|\xi|^2$, where $\xi \equiv \vec{\xi}\cdot\vec{\nabla}\psi$ is proportional to the *displacement of a fluid element in the direction normal to a* magnetic surface. This allows the two components of $\vec{\xi}$ within the surface to be eliminated analytically [14], thus reducing matrix sizes by a factor of 3 and making calculations at $n \sim 20$ feasible.

At first sight, the use of a model kinetic energy seems undesirable since the resulting growth rates are nonphysical. However, the <u>sign</u> of ω^2 is independent of normalization, and for calculating marginal stability points, *our choice is actually much* more practical because $\omega^2(\beta, n)$ is an analytic function near $\omega^2 = 0$. In contrast, $\omega^2 = 0$ is the lowest point of a continuum.

band when the physical kinetic energy $(1/2)\rho\omega^2|\vec{\xi}|^2$ is used, making accurate extrapolation to marginal stability difficult.

After Bineau reduction [14], the Euler-Lagrange equation is

$$(\rho\omega^2 + F)\ \xi = 0\ , \tag{3}$$

where the scalar operator F is defined, for $n \neq 0$, by

$$F = \left(\vec{B}\cdot\vec{\nabla}\ \frac{\vec{\nabla}\psi}{|\vec{\nabla}\psi|^2} + \frac{\vec{j}\times\vec{\nabla}\psi}{|\vec{\nabla}\psi|^2}\right)\cdot\vec{\nabla}\Delta_s^{-1}\vec{\nabla}\cdot\left(\frac{\vec{\nabla}\psi}{|\vec{\nabla}\psi|^2}\ \vec{B}\cdot\vec{\nabla} - \frac{\vec{j}\times\vec{\nabla}\psi}{|\vec{\nabla}\psi|^2}\right)$$
$$+\ \vec{B}\cdot\vec{\nabla}\ \frac{1}{|\vec{\nabla}\psi|^2}\ \vec{B}\cdot\vec{\nabla} + 2K\ , \tag{4}$$

where $\vec{j}$ is the equilibrium current density, Δ_s^{-1} is the Green's function operator which inverts the surface Laplacian

$$\Delta_s \equiv \vec{\nabla}\cdot\left(\overleftrightarrow{I} - \frac{\vec{\nabla}\psi\vec{\nabla}\psi}{|\vec{\nabla}\psi|^2}\right)\cdot\vec{\nabla}\ , \tag{5}$$

and

$$K \equiv \frac{\vec{j}\times\vec{n}\cdot(\vec{B}\cdot\vec{\nabla}\vec{n})}{|\vec{\nabla}\psi|^2}\ , \tag{6}$$

where $\vec{n} \equiv \vec{\nabla}\psi/|\vec{\nabla}\psi|$.

In axisymmetric geometry we assume a normal mode to go as $\exp(-in\zeta)$, so that Δ_s reduces to a second order <u>ordinary</u> differential operator in θ. Its inversion can, therefore, be done surface by surface. We solve Eq. (3) by Galerkin's method [13], using a truncated Fourier representation in θ, and finite elements in ψ. The calculations were performed on the NMFECC CRAY-I computer using 51 Fourier modes and 72 radial elements. The equilibria were calculated on a 129×129 rectangular X-Z grid, and mapped onto a 145×256 $\psi-\theta$ grid using high order spline interpolation. The results for sequences I and II are represented in Fig. 1.

V. WKB FORMALISM

This is a development of the ballooning mode formalism [2-5], which uses $\varepsilon \equiv 1/n$ as an expansion parameter to develop an asymptotic solution of Eq. (3). Ordering ω^2 finite (so that ω^2 can be negative), and looking at the asymptotic limit $\varepsilon \to 0$, we see that $\vec{B}\cdot\vec{\nabla}\xi$ must be O(1). The eikonal representation

$$\xi = \hat{\xi}(\theta,\psi,\alpha,\varepsilon)\ \exp[-i\omega t - iS(\alpha,\psi)/\varepsilon] \tag{6}$$

satisfies this, with [2] $\alpha \equiv \zeta - q\theta$ so that $\vec{B} = \vec{\nabla}\alpha \times \vec{\nabla}\psi$. In the axisymmetric case, S is separable

$$S(\alpha,\psi) = \alpha + \int k_q(\psi)\ dq\ (\psi) \tag{7}$$

where k_q/ε is the radial wavenumber in $\alpha - q$ coordinates. By our choice of "straight field line" coordinates, we have avoided the need for an eikonal description of the fast θ-dependence [5].

As always in WKB theory, Eq. (6) applies only on a single branch of the dispersion relation. The physical solution is to be found by linear superposition of all branches having the same frequency, with amplitudes and phases chosen to satisfy boundary conditions and turning point matching conditions. Thus the fact that Eq. (6) does not satisfy periodicity in θ is irrelevant at this stage.

Inserting Eq. (6) into Eq. (3), and expanding in powers of ϵ, we find at lowest order

$$\left(\rho\omega^2 + \vec{B}\cdot\vec{\nabla} \frac{|\vec{k}|^2}{B^2} \vec{B}\cdot\vec{\nabla} + \frac{2p'(\psi)}{B^2} \vec{k} \times \vec{\kappa}\cdot\vec{B} \right) \hat{\xi}^{(0)} = 0 \quad , \tag{8}$$

where $\vec{\kappa}$ is the field line curvature, p is the pressure, and $\vec{k}/\epsilon$ is the wavevector $\vec{\nabla}S/\epsilon$. That is, for an axisymmetric system,

$$\vec{k} = \vec{\nabla}\alpha + k_q\vec{\nabla}q = \vec{\nabla}\zeta - q\vec{\nabla}\theta + (\theta - k_q)\ \vec{\nabla}q \quad . \tag{9}$$

Note that $\vec{k}\cdot\vec{B} = 0$, whereas $\vec{k}\cdot\vec{\nabla}\psi$ increases secularly as $\theta \rightarrow \pm\infty$.

Equation (8) is to be solved as an eigenvalue equation for ω^2 under the condition [5] that $\hat{\xi}^{(0)}$ be square integrable on the domain $-\infty < \theta < \infty$, thus yielding the dispersion relation $\omega^2 = \lambda(\psi, k_q)$. Although k_q plays a similar role to the parameter η_o occurring in Ref. 5, it is here clearly a function of ψ , since ω^2 = const for a normal mode. The fact that k_q occurs in Eq. (8) only in the combination $(\theta - k_q)$ implies [8] that λ is <u>a periodic function of</u> k_q (period 2π). Thus there is an infinity of degenerate branches of the dispersion relation, which allows us to form a periodic normal mode by using an infinite sum of these solutions [3-5].

Figure 2 shows typical contours of constant $\lambda(q, k_q)$ over a half period in k_q, and over the band of unstable surfaces, $q_L < q(\psi) < q_R$. As will become apparent [see Eq. (11)], it is here convenient to label surfaces by q rather than ψ . The outermost contour is at marginal stability, $\lambda = 0$. The inner contours are equally spaced in λ between 0 and the most unstable value $\lambda_{min}(<0)$. As β increases, the area enclosed by the $\lambda = 0$ contour increases. In fact, for sufficiently high β, the $\lambda = 0$ contour in the range $-\pi < k_q < \pi$ coalesces with the $\lambda = 0$ contours in the neighboring ranges (see Fig. 3), and the value of λ at the saddle point at (q_x, π) becomes negative. This topological complication will not be treated here.

Thus, we assume that the two branches in the range $-\pi < k_q < \pi$ couple only with each other, at the turning points $q = q_L$ and $q = q_R$. The ε-expansion breaks down near a turning point, but an expansion in $\varepsilon^{1/3}$ can be used instead, and the resultant Airy function solution matched to the incident and reflected waves. In traditional WKB fashion [15] the phase change is found to be $\pi/2$ at a turning point, thus yielding [8] the "quantization" condition for the radially extended eigenmodes

$$n \oint k_q \, dq = 2\pi(N + 1/2) \ , \tag{10}$$

where N = 0, 1, 2, ... Although N should strictly be O(n) for the WKB theory to apply, it is well known that Eq. (10) is exact for a harmonic oscillator potential at all N, and we, therefore, assume Eq. (10) to be a good approximation even at $N = 0$, which is the mode of highest growth rate. Thus we estimate the value of n at which the most unstable mode stabilizes to be

$$n_c = \pi \Big/ \oint k_q \, dq \quad , \tag{11}$$

where $\oint k_q \, dq$ is the area enclosed by the $\lambda = 0$ contour in the $q - k_q$ plane. The result of applying Eq. (11) to sequences I and II is shown in Fig. 1. The curves are continued down to $n_c = 5$.

This formula reduces to the $1/n$ correction formula [5,6] when $\lambda(q, k_q)$ in the range $0 \geq \lambda \geq \lambda_{min}$ can be approximated by Taylor expanding to second order in $(q - q_o)$ and $(k_q - k_q^o)$, where (q_o, k_q^o) is the location of the $\lambda = \lambda_{min}$ point. We find

$$n_c \approx \frac{1}{2|\lambda_{min}|} \left(\frac{\partial^2 \lambda}{\partial q^2} \frac{\partial^2 \lambda}{\partial k_q^2} \right)_o^{1/2} \quad . \tag{12}$$

The fact that $\lambda = 0$ contour in Fig. 2 is not elliptical indicates that the Taylor expansion is breaking down. However, application of Eq. (12) to the case shown in Fig. 2 ($\beta \simeq 10.5\%$) gives $n_c \simeq 26$, compared with $n_c \simeq 18$ from application of Eq. (11). Thus nonellipticity of the $\lambda = 0$ contour is not in itself sufficient to explain the order of magnitude discrepancy with the result of Ref. 1, $n_c \simeq 150$.

We have also calculated the λ-contours with $\rho\omega^2$ in Eq. (2) replaced by $\rho\omega^2|\vec{k}|^2/B^2$, which is the model normalization used in Refs. 2 and 5. This models the physical kinetic energy better than our model, but has the mathematical disadvantage that it generates a continuous spectrum for $\lambda \geq 0$. Thus the Taylor expansion used to derive Eq. (12) must fail to converge at or before $\lambda = 0$, and the approximation of retaining the first three terms may be wildly inaccurate. This is confirmed by the fact that this model normalization gives $n_c \approx 62$ for the 10.5% β case referred to above. Even this result is less than that of Ref. 1 by a factor of more than 2. This discrepancy can probably be ascribed to the use in Ref. 1 of an orthogonal coordinate system, which gives rise to severe numerical difficulties [16]. This is because of an accidental vanishing of the local shear ν' near the most unstable surface. In "straight field line" coordinates, such as those we use, ν' does not occur in Eq. (12), and no such problem arises.

VI. DISCUSSION

The agreement between the two methods for $n \gtrsim 5$, as shown in Fig. 1, is quite impressive and builds confidence in the accuracy of both. However, the simple WKB theory of Sec. V fails to predict the oscillatory structure at low n revealed by the PEST-II results. The oscillations can be understood qualitatively as due to the movement of rational surfaces relative to the band of ballooning unstable surfaces, as illustrated in Figs. 4 and 5. The growth rate is found empirically to peak when $q_x = m/n$, where m is an integer and q_x is the value of q at the saddle point occurring at $k_q = \pi$ in the $\lambda(q, k_q)$ contour plots (Fig. 3). This is also approximately true when $\lambda(q_x, \pi) > 0$, but if the unstable region is localized close to $k_q = 0$, as occurs at low β, the amplitude of the oscillations is very small and m/n is closer to q_o. The oscillatory structure can be explained by an extension of the WKB formalism to include tunneling between different branches.

Although fractional values of n are not physically realizable, $\beta_c(n)$ is an analytic function and can be extrapolated. However, since the period of the oscillations is $\Delta n \simeq 1/q_x < 1$, extrapolation based only on integer values of n is not a valid procedure. Also, q_x is a function of equilibrium parameters, and the behavior of the curve at fractional n is a good indicator of the sensitivity of the results to small changes in the equilibrium.

Sequence II appears to have superior stability properties to Sequence I at intermediate values of n, presumably due to stronger shear, but the $n = \infty$ limit on β_c is approximately the same for both. (In fact, $\beta_c(\infty)$ is somewhat lower in Sequence II.) Even for Sequence II, when β is significantly greater than $\beta_c(\infty)$, there is a broad band of unstable modes with $k_\perp \rho_i < 1$. The effect of such modes on transport must be determined before the significance of this result for high β tokamak operation can be evaluated.

More details on PEST-II and on the WKB formalism will be published elsewhere.

ACKNOWLEDGMENTS

We wish to acknowledge Dr. A. M. M. Todd for his assistance in generating the equilibria, Mr. A. E. Miller for performing many of the PEST-II runs, Drs. A. H. Glasser, J. M. Greene, and E. A. Frieman for sharing their knowledge of ballooning modes, and Dr. D. A. Monticello for stimulating our interest in the sequences studied.

This work was supported by United States Department of Energy Contract No. DE-AC02-76-CHO-3073.

REFERENCES

[1] L. A. Charlton, R. A. Dory, Y.-K. M. Peng, D. J. Strickler, S. J. Lynch, D. K. Lee, R. Gruber, and F. Troyon, Phys. Rev. Lett. 43, 1395 (1979).

[2] D. Dobrott, D. B. Nelson, J. M. Greene, A. H. Glasser, M. S. Chance, and E. A. Frieman, Phys. Rev. Lett. 39, 943 (1977).

[3] A. H. Glasser, Proceedings of the Finite Beta Theory Workshop, Varenna, 1977, B. Coppi and W. Sadowski, eds. (U. S. Dept. of Energy, CONF-7709167, 19,7), p. 55.

[4] Y. C. Lee and J. W. Van Dam, Varenna, 1977 (as in Ref. 3), p. 93.

[5] J. W. Connor, R. J. Hastie, and J. B. Taylor, Proc. R. Soc. Lond. A365, 1 (1979).

[6] M. S. Chance, R. L. Dewar, E. A. Frieman, A. H. Glasser, J. M. Greene, Y-Y. Hsieh, J. L. Johnson, J. Manickam, and A. M. M. Todd, Proceedings of the Sherwood Meeting, Gatlinburg, 1978 (Oak Ridge National Laboratory, 1978), Abstract OB1.

[7] R. C. Grimm and R. L. Dewar, _Proceedings of the Sherwood Meeting_, Mt. Pocono, 1979 (Princeton Plasma Physics Laboratory, 1979), Abstract 3B38.

[8] R. L. Dewar, M. S. Chance, A. H. Glasser, J. M. Greene, and E. A. Frieman, Princeton Plasma Physics Laboratory Report PPPL-1587 (1979).

[9] _U. S. INTOR, The U. S. Contribution to the International Tokamak Reactor Workshop_, W. M. Stacey, Jr. ed. (1979), Summary p. 2.

[10] R. A. Dory and Y.-K. M. Peng, Nucl. Fusion _17_, 1 (1977).

[11] R. G. Bateman and Y.-K. M. Peng, Phys. Rev. Lett. _38_, 829 (1977).

[12] L. A. Charlton, private communication.

[13] R. C. Grimm, J. M. Greene, and J. L. Johnson, in _Methods in Computational Physics_, Vol. 16, J. Killeen, ed. (Academic, N. Y., 1976) p. 253.

[14] M. Bineau, Nucl. Fusion _2_, 130 (1962).

[15] P. M. Morse and H. Feshbach, Methods of Theoretical Physics (McGraw-Hill, New York, 1953), p. 1099.

[16] L. A. Charlton, D. B. Nelson, and R. A. Dory, Oak Ridge National Laboratory Report ORNL/TM-7198 (1980).

FIGURE CAPTIONS

Fig. 1. β_c vs $1/n$ for Sequences I and II. Solid line connects PEST-II results, dashed line connects results from Eq. (11). The large dots are additional PEST-II points. In Sequence II, the values of β were obtained using the approximation $\beta \simeq 21\%/s^2$, which overestimates β for the diamagnetic plasma considered here.

Fig. 2. Contours of constant $\lambda(q, k_q)$ for the case $s = 1.414$ ($\beta \simeq 10.5\%$) in Sequence II, plotted at nine equal levels between 0 (outermost contour, $q_L < q < q_R$) and λ_{min} [most unstable point, at $(q_o, 0)$].

Fig. 3. Contours of constant λ for the case $\beta = 8.9\%$ of Sequence I, which is a case where the saddle point at (q_x, π) is unstable [$\lambda(q_x, \pi) < 0$]. This topological configuration occurs for $\beta > 8\%$ in Sequence I, and $\beta > 18\%$ in Sequence II.

Fig. 4. Fourier amplitudes of a mode with $n = 6.5$ for the case $\beta = 7.5\%$ of Sequence I. The strongest component ($m = 7$) satisfies the relation $m \simeq nq_x$. This case is typical of those with maximum growth rate (minimum β_c). The locations of some rational surfaces are shown.

Fig. 5. Fourier amplitudes of a mode with n = 6.9 for the case β = 7.5% of Sequence I. The strongest component (m = 8) satisfies the relation $m - 1/2 \simeq nq_x$. This case is typical of those with minimum growth rate (maximum β_c).

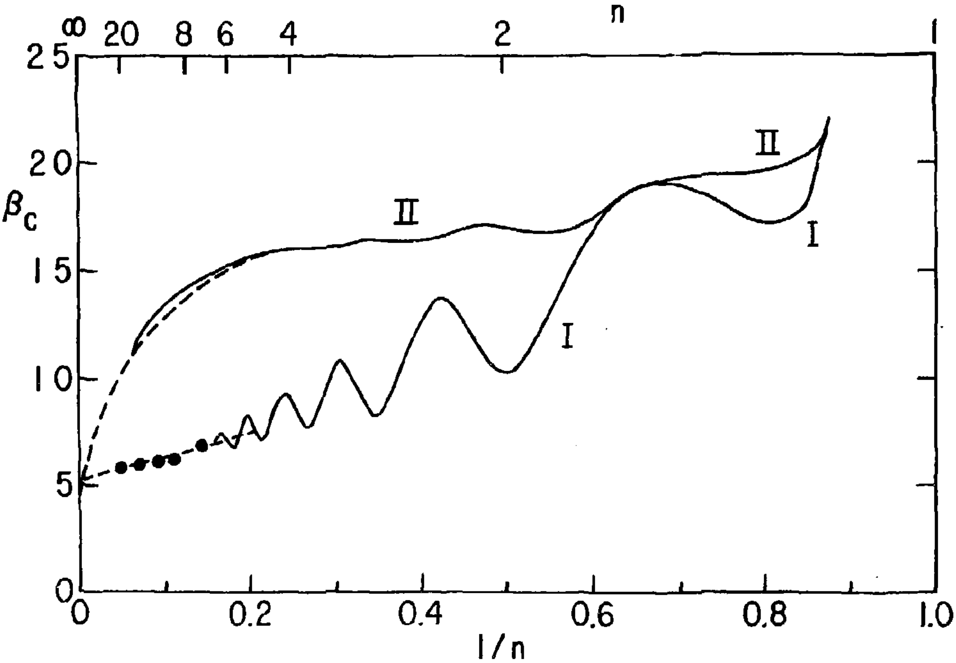

Fig. 1. (PPPL-802128)

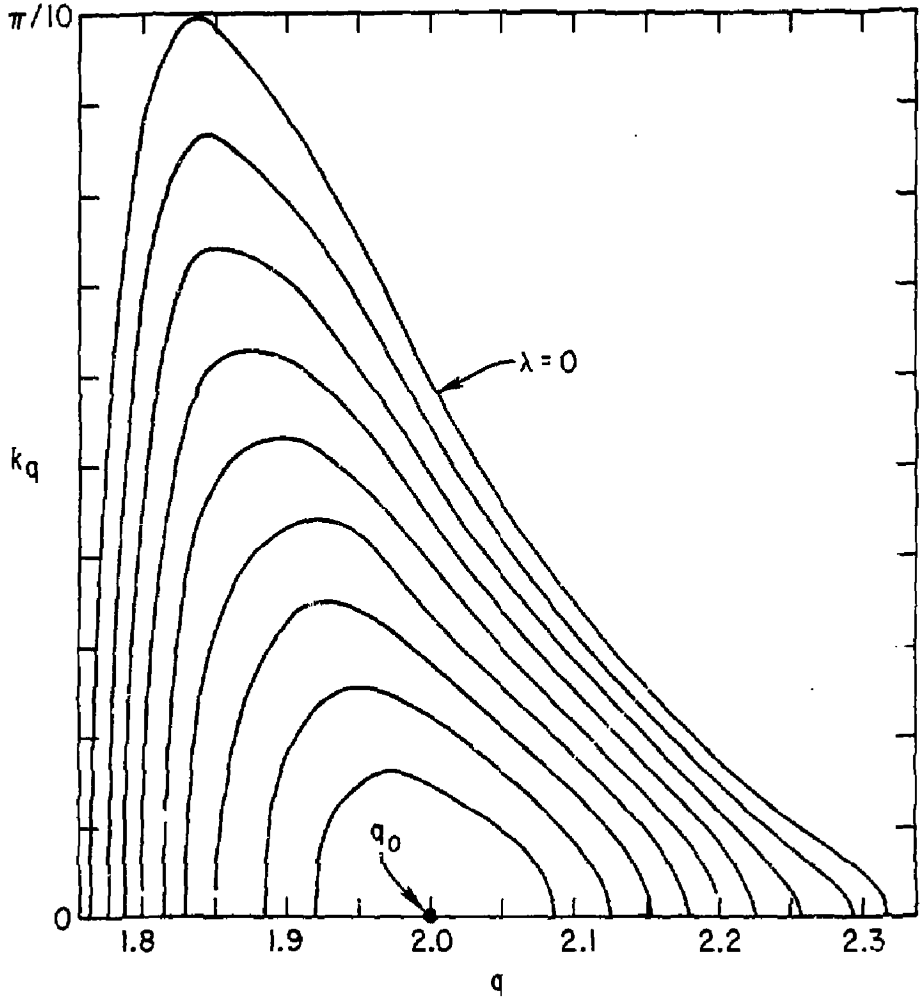

Fig. 2. (PPPL-802092)

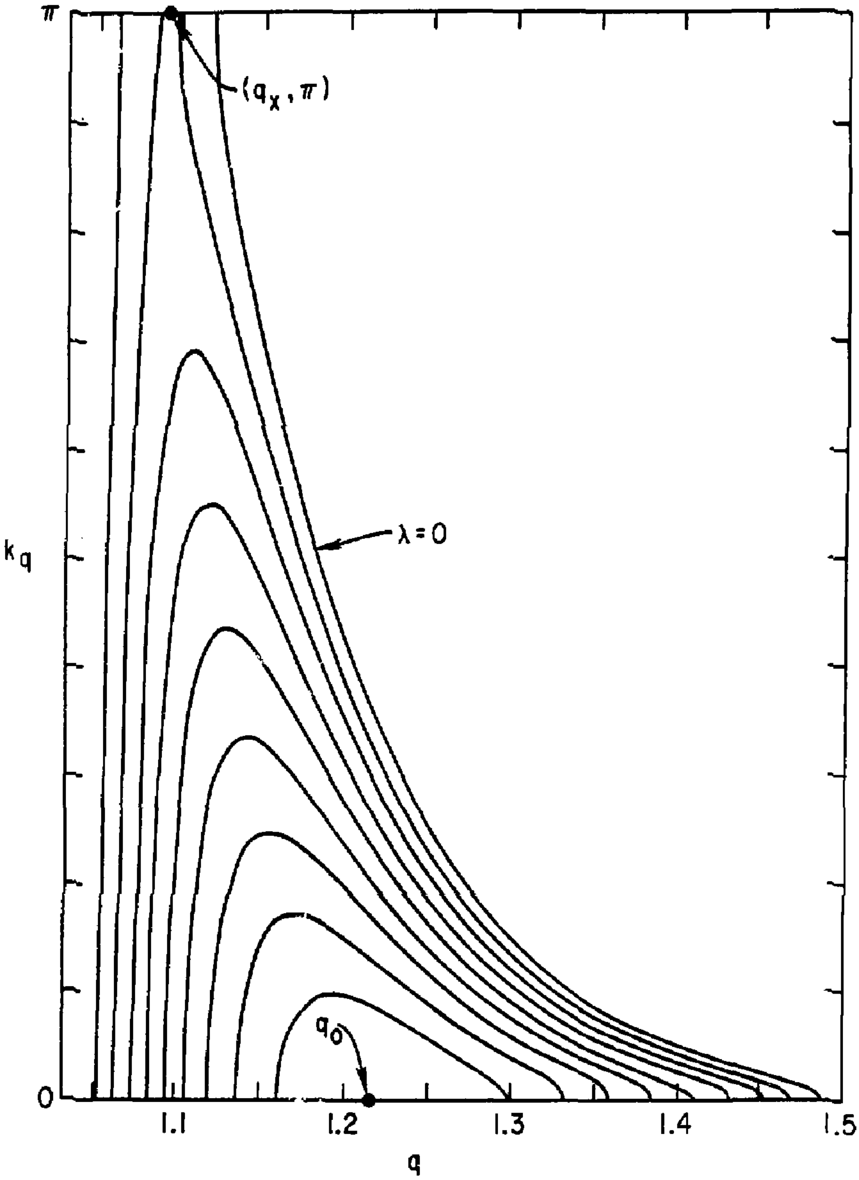

Fig. 3. (PPPL-802091)

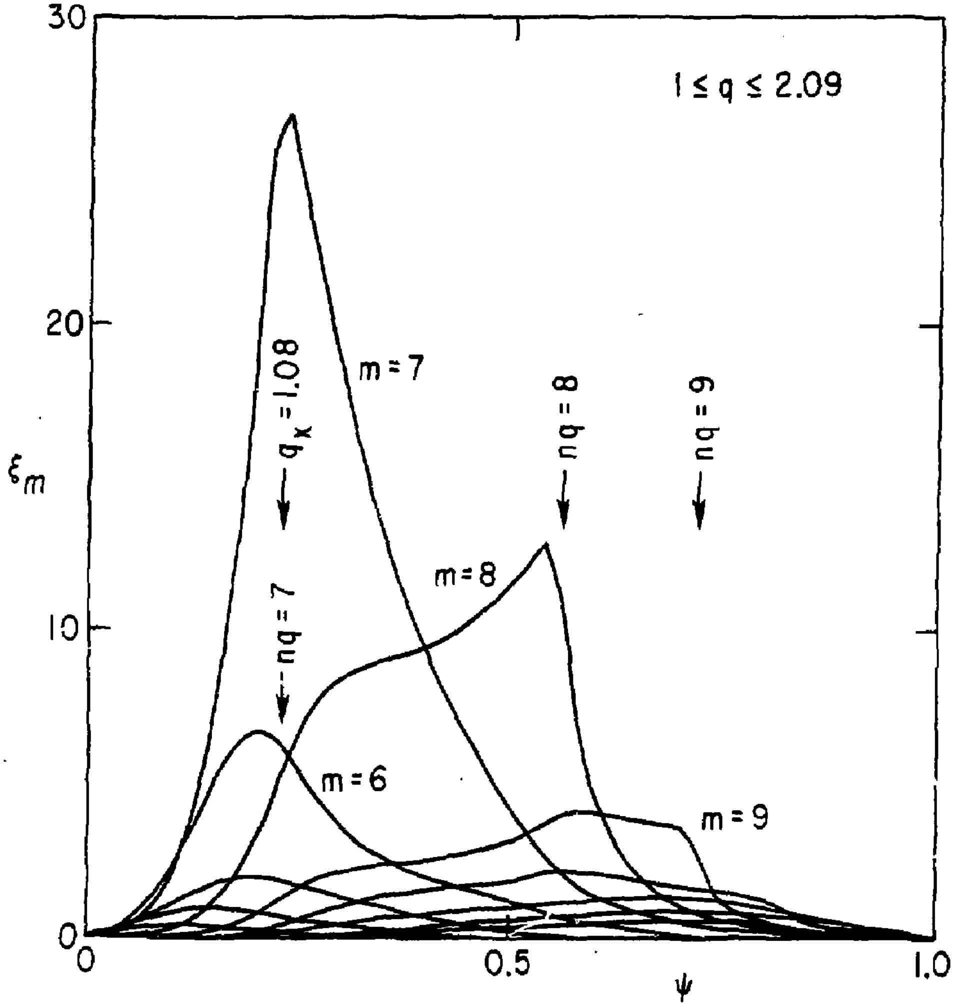

Fig. 4. (PPPL-802127)

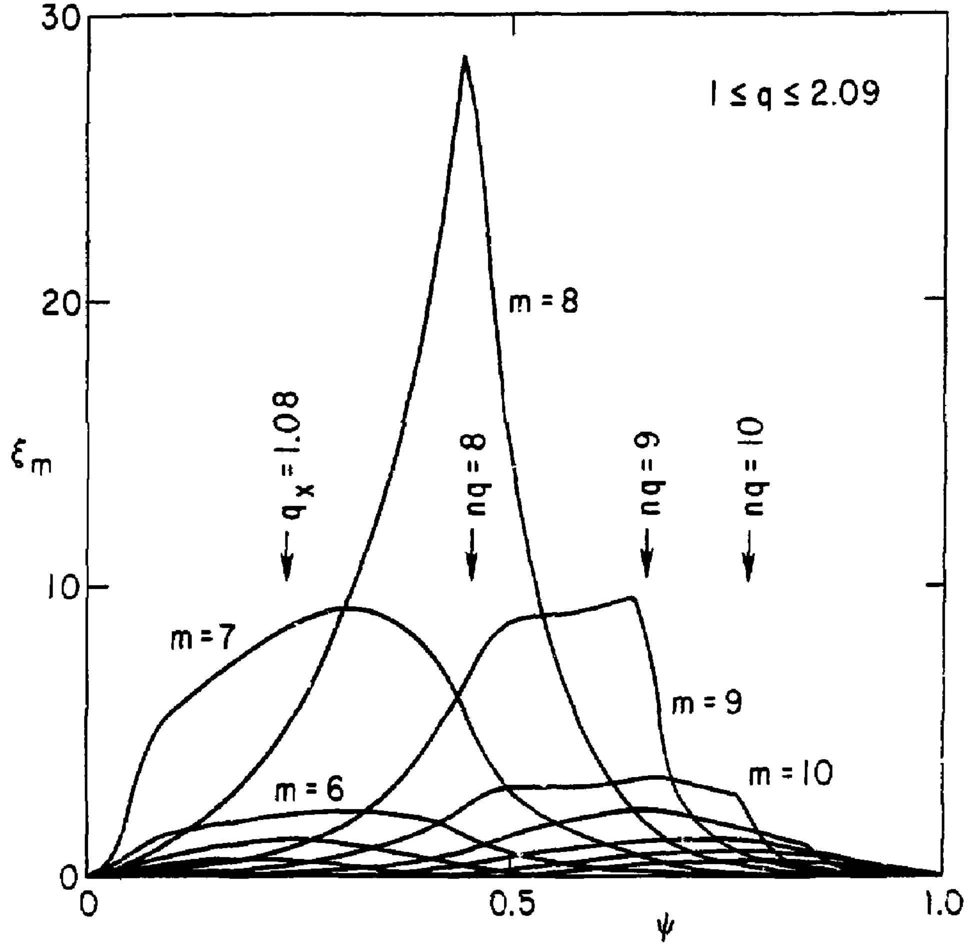

Fig. 5. (PPPL-802126)